A novel second-order nonlinear optical guest–host polymeric material exhibiting optical transparency down to 400 nm

Rong-Ho Lee[a], Ging-Ho Hsiue[a,*], Ru-Jong Jeng[b]

[a]Department of Chemical Engineering, National Tsing Hua University, Hsinchu, 300 Taiwan, ROC
[b]Department of Chemical Engineering, National Chung Hsing University, Taichung, 400 Taiwan, ROC

Abstract

A guest–host system of a nonlinear optical (NLO) arylphosphine oxide and polyhydroxystyrene (PSOH) has been investigated for second-order nonlinear optics. The synthesized NLO-active arylphosphine oxides show spectroscopic properties in accordance with the proposed structures using n.m.r. spectrometry. These NLO-active arylphosphine oxides and polymer matrix exhibit optical transparency down to 400 nm, and excellent thermal stability ($T_d > 345°C$). An NLO-active chromophore with short absorption wavelength is desirable for application in frequency doubling. Moreover, the excellent thermal stability of the chromophore will prevent its decomposition during the poling process at elevated temperatures. The homogeneity of these guest–host NLO polymers are confirmed using scanning electron microscopy (SEM). The second-order nonlinearity and temporal stability of these NLO polymers were also reported. The relationship between molecular motion and temporal stability are studied by dielectric analysis. © 1998 Elsevier Science Ltd. All rights reserved.

Keywords: Second-order nonlinear optical; Optical transparency; Dielectric relaxation

1. Introduction

Second-order nonlinear optical (NLO) polymers have been widely studied for applications in frequency doubling and electro-optical (EO) modulation [1,2]. The polymers show second-order NLO effects when the NLO-active chromophore is oriented in a noncentrosymmetric structure by an electric poling process. Moreover, large second-order nonlinearity can be obtained for the NLO polymer containing a chromophore consisting of strong electron-donating and -withdrawing groups separated by a π-delocalized moiety. These NLO-active polymers typically have longer cutoff wavelengths in absorption. The long cutoff wavelengths result in resonant enhancement of the second harmonic signal [1]. However, resonant enhancement should be avoided for frequency doubling. This is because of the fact that the optical power density in most NLO waveguide devices is quite large. A small absorption can cause intolerable damage for NLO polymers [1]. Therefore, the optical transparency down to a lower cutoff wavelength is an important consideration in designing second-order NLO polymers for frequency doubling.

Recently, a few NLO organic materials with desirable

optical transparency have been investigated [3–9]. One group of these materials is the NLO-active substituted arylphosphine oxides [7–9]. The NLO-active substituted arylphosphine oxides exhibit a cutoff wavelength shorter than 350 nm [7–9]. The fact that no absorption in the region where diode laser-driven second harmogenic generation (SHG) occurs is desirable for frequency doubling [5]. Moreover, the substituted arylphosphine oxides have excellent thermal stability [7]. This will prevent the decomposition of the phosphine oxide during the corona poling process for their use as NLO-active chromophores in the polymer matrix. In addition, the hydrogen-bonding between the donor (substituted) group and electron-withdrawing phenylphosphine oxide is a beneficial characteristic in second-order NLO materials [7,10–12]. This is favourable for the formation of the noncentrosymmetric structure. Therefore, the substituted arylphosphine oxide is a good candidate to be an NLO-active chromophore. Desirable optical transparency and environmental stability of the NLO polymers will be obtained when the NLO-active substituted arylphosphine oxide is incorporated into the polymeric matrix.

In this study, the NLO-active tris(3-nitrophenyl)-phosphine oxide (TNPO) and tris(3-aminophenyl)-phosphine oxide (TAPO) were synthesized. These two NLO-active chromophores were separately doped into the

* Corresponding author.

polyhydroxystyrene (PSOH). PSOH was chosen because there could be intermolecular hydrogen-bonding between the NLO-active chromophore and polymer [7,10–12]. Therefore, a high doping level of the NLO-active chromophore was achieved for this guest–host system. Phase homogeneity of these guest–host NLO polymeric materials were confirmed using scanning electron microscopy (SEM). The second-order nonlinearity was obtained by an applied electric poling field. The temporal stability of second-order optical nonlinearity was observed at 35 and 100°C via in situ second-harmonic generation technique. Moreover, the thermal dynamic behaviours were studied by using broadband dielectric relaxation spectroscopy. The influence of the molecular motion on the temporal stability of second-order nonlinearity was also discussed.

2. Experimental

2.1. Synthesis of TNPO and TAPO

The synthesis of TNPO and TAPO is shown in Scheme 1. TNPO and TAPO were obtained via the nitration and subsequent reduction of triphenylphosphine oxide. The chemical structures of TAPO and TNPO were confirmed using a Bruker MSL-300 (300 MHz) NMR spectrometer. PSOH was obtained from Aldrich ($M_n = 30\,000$ g mol^{-1}) and was used as received.

A solution of sulfuric acid (15 ml) and nitric acid (6.3 g) was added dropwise over a period of 30 min into a stirred solution of triphenylphosphine oxide (5 g) in sulfuric acid (100 ml) at 0°C, and the solution was allowed to rise to room temperature after 5 h. The solution was then added into the water. The precipitate was extracted with ethyl acetate and washed with bicarbonate aqueous solution until neutral pH was reached. The solvent was then removed. The solid residue was recrystallized from mixed solvent (ethyl acetate and n-hexane). TNPO was obtained with a 87% yield. ^1H n.m.r. (d-DMSO) δ 7.99–8.06 (m, 3H), 8.28–8.35 (m, 3H), 8.58–8.67 (m, 6H).
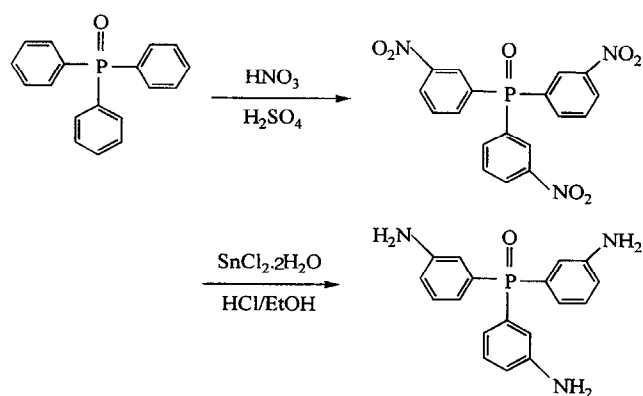
Scheme 1.

TNPO (1.5 g) was reacted with powdered tin(II) chloride dihydrate (6.5 g) in a solution of 75 ml ethanol and 75 ml fuming hydrochloric acid at room temperature for 8 h. The solution was neutralized with 25% NaOH aqueous solution. The raw product was then extracted with ethyl acetate. After removing the solvent, the solid residue was recrystallized from mixed solvent (ethyl acetate and n-hexane) to give a pure product. The TAPO was obtained with a 72% yield. ^1H n.m.r. (d-DMSO) δ 6.93–6.97 (d, 3H, P–C=CH–C–NH2), 5.45 (s, 6H, P–C=CH–C–NH2), 6.70–6.76 (m, 3H, P–C–CH=CH–CH), 7.19–7.25 (m, 3H, P–C–CH=CH–CH), 6.80–6.84 (d, 3H, P–C–CH=CH–CH); ^{13}C n.m.r. (d-DMSO) δ 133.32, 134.66 (P–C–CH=CH), 116.41, 116.55 (P–C=CH–C–NH2), 148.65, 148.83 (P–C=CH–C–NH2), 118.59, 118.72 (P–C–CH=CH–CH), 128.79, 128.97 (P–C–CH=CH–CH), 116.74, 116.76 (P–C–CH=CH–CH); ^{31}P n.m.r. (d-DMSO) δ 28.84 (C–P=O).

2.2. Preparation of guest–host samples

The guest–host samples (TNPO/PSOH and TAPO/PSOH) with different weight ratios (sample TNPO10, 10:90; sample TAPO25, 25:75) were prepared for NLO measurements. The doping levels for TNPO/PSOH and TAPO/PSOH were obtained from the highest content of NLO dyes in polymers without formation of dye aggregation [13]. TNPO10 was obtained by dissolving TNPO (0.01 g) and PSOH (0.09 g) in N,N-dimethylformamide (DMF, 2 ml). Moreover, the polymer solution of TAPO25 containing TAPO (0.025 g) and PSOH (0.075 g) in DMF (1 ml) was also prepared for film fabrication. Thin film was prepared by spin coating the polymer solution onto indium tin oxide (ITO) glass substrates.

2.3. Physical characterization

Thermal behaviour of these NLO-active chromophores and guest–host polymeric materials were determined by the differential scanning calorimeter (d.s.c.; Seiko SSC/5200) with a heating rates of 10°C min^{-1}. Glass transition temperature (T_g) was read at the middle of the change in heat capacity. The transitions were collected from the second heating scan. Thermal degradation temperature (T_d) was measured using DuPont 951 thermogravimetric analyser (t.g.a.) at 10°C min^{-1} under air. The temperature at weight loss of 5% was defined as T_d. U.v.-vis spectra were recorded on a Hitachi 320 spectrophotometer. SEM (Jeol JEM-840A) was employed to study the morphology of the polymer film which was coated with a thin layer of carbon. In addition, dielectric relaxation behaviour of the NLO polymers was studied by dielectric spectroscopy (DEA; Novercontrol GmbH). The measurement was performed using a Schlumberger SI1260 impedance/gain-phase analyser and a Quator temperature controller. Dielectric measurements were performed from −40 to 150°C. The frequency scan range was from 10^{-1} to 10^6 Hz.

2.4. Corona poling process and NLO measurement

The poling process for the second-order NLO polymer films was carried out using an in situ poling technique. The details of the corona poling set-up were the same as was reported earlier [14]. The poling process was started at room temperature and then the temperature was increased up to 125°C with a heating rate of 5°C min^{-1}. The corona current was maintained at 1.5 μA with a potential of 4.5 kV, while the poling temperature was kept at 125°C for 40 min. Upon saturation of the SHG signal intensity, the sample was then cooled down to room temperature in the presence of the poling field. Once room temperature was reached, the poling field was terminated. The thickness and indices of refraction were measured using a prism coupler (Metricon 2010). The typical thickness obtained was approximately 0.73 and 0.86 μm for TNPO10 and TAPO25, respectively. The indices of refraction were 1.68 (532 nm) and 1.60 (1064 nm) for TNPO10. For TAPO25, 1.67 (532 nm) and 1.58 (1064 nm) were obtained. Second harmonic generation measurements were carried out with a Q-switched Nd:YAG laser operating at 1064 nm. The relaxation behaviour of the second-order NLO properties was studied by monitoring the decay of the effective second-order NLO coefficient, d_{eff}, as a function of time at 35 and 100°C. The measurements of the second harmonic coefficient, d_{33}, have been previously discussed [15] and the d_{33} values were corrected for absorption [16].

3. Results and discussion

Heteronuclear chemical shift correlation (HETCOR) spectrum of TAPO is shown in Fig. 1. ^{1}H–^{13}C correlation is revealed by a crosspeak contour at the intersection of a horizontal line drawn from a proton peak and a vertical line drawn from a ^{13}C peak. The coupling of carbon and phosphorus atoms leads to the splitting of the absorption peak, to be a doublet, for all of the ^{13}C peaks in spectrum. The carbon atoms attached to the phosphorus atom and amino group show two pairs of doublets at δ 133.32, 134.66 and 148.65, 148.83, respectively. These two pairs of ^{13}C peaks show no crosspeak contour with proton peaks. In the ^{1}H spectrum, the absorption peak of the protons (H-5 and H-6 protons) in amino group is shown at δ 5.45. Moreover, the protons (H-1, H-2, H-3, and H-4) show doublets and multiplets in the spectrum. These absorption peaks split into doublets or multiplets due to the coupling of the proton–proton and proton–phosphorus atoms. These proton peaks show four crosspeaks with the ^{13}C peak of each proton attached to carbon atoms in this HETCOR spectrum. It is concluded that the spectroscopic properties of the TAPO is in accordance with the proposed structure.

The absorption characteristics of the NLO-active chromophore and polymer matrix were studied by u.v.-vis spectroscopy. The u.v./vis absorption spectra of chromophores TNPO, TAPO and polymer PSOH in THF are shown in Fig. 2. PSOH has a cutoff wavelength (λ_{cutoff})

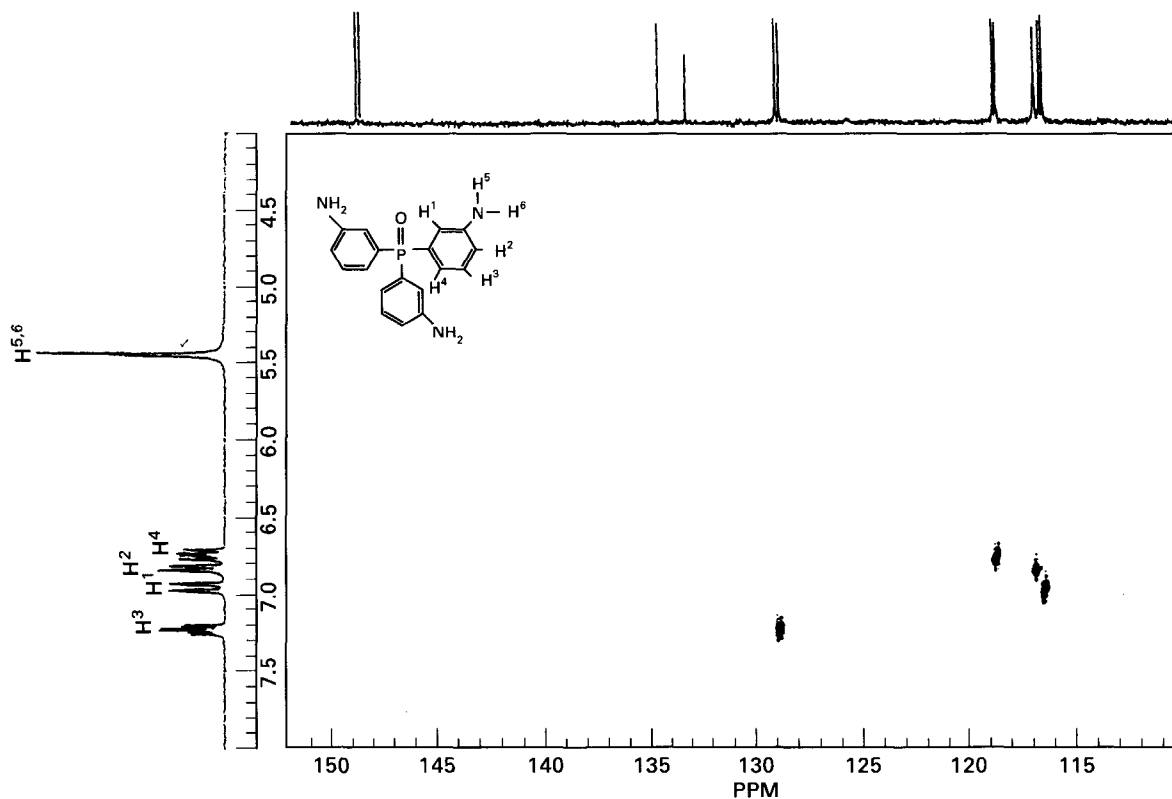
Fig. 1. Heteronuclear chemical shift correlation (HETCOR) spectrum of TAPO.

at 398 nm. For TNPO, the wavelength of maximum absorption (λ_{max}) and cutoff wavelength were observed at 255 and 325 nm, respectively. Moreover, the λ_{max} and λ_{cutoff} were, respectively, observed at 310 and 350 nm for TAPO. The U.v./vis spectra show that the NLO-active substituted arylphosphine oxides and PSOH have a cutoff wavelength absorption shorter than 400 nm. An NLO-active material with short absorption wavelength is desirable for the frequency doubling application.

The optical qualities of the polymer films have been confirmed using optical microscopy. No sign of any phase separation was observed when the magnification was increased up to 1.6 K for samples TAPO25 and TNPO10. In addition, the homogeneity of these guest–host NLO polymers was further investigated using SEM. The distribution of the guest molecules (TNPO or TAPO) in polymer matrix was observed using a mapping technique [17]. The X-ray elemental maps of samples TNPO10 and TAPO25 are shown in Fig. 3(a) and Fig. 3(b), respectively. The bright points in the micrographs represent the locations of the phosphorus element in the polymer film [17]. This result indicates that the guest molecules are distributed uniformly in the polymer matrix for samples TNPO10 and TAPO25. The particle sizes of the arylphosphine oxides are smaller than 1 μm. No aggregation of the aryphosphine oxides was observed, even though a large quantity (25% by weight) of guest molecules was doped into the polymer film. High miscibility of the substituted arylphosphine oxide and PSOH was possibly due to the fact that these two respective components possess strong polar functional groups, which

leads to intermolecular hydrogen-bonding between the guest molecules and polymer host [7,10–12].

T_g values of PSOH, TNPO10, and TAPO25 were determined by d.s.c. PSOH has a T_g of 147.5°C. T_g values were observed at 101.2 and 78.6°C for samples TNPO10 and TAPO25, respectively. A plasticizer effect results in a lower T_g values for samples TNPO10 and TAPO25 compared to PSOH. T_d values of samples PSOH, TNPO10, and TAPO25 were determined by t.g.a. T_d values for PSOH, TNPO10, and TAPO25 are 362.5, 307.1 and 337.5°C, respectively. Moreover, T_d values for NLO-active chromophores TNPO and TAPO were observed at 348.2 and 354.8°C. The NLO-active arylphosphine oxides have a higher degradation temperature as compared to azo- and stilbene-conjugated NLO chromophores. This type of chromophore, exhibiting excellent thermal stability, can be utilized in the highly thermally stable NLO polymeric system, such as EO polymers [18,19].

The temporal stability of second-order optical nonlinearity is related to the molecular mobility of polymer chains for a guest–host NLO polymeric system. Broadband dielectric spectroscopy is useful in studying the relaxation behaviour of the NLO polymers [20]. The temperature dependence of dielectric loss tangent for samples PSOH, TNPO10, and TAPO25 are shown in Fig. 4(a–c), respectively. In Fig. 4(a), the α- and β-relaxations were observed at low frequency range. The α-relaxation is the process associated with the glass transition; with the β-relaxation corresponding to the local motion of the twisting of the polymer main chains [21]. This relaxation was only
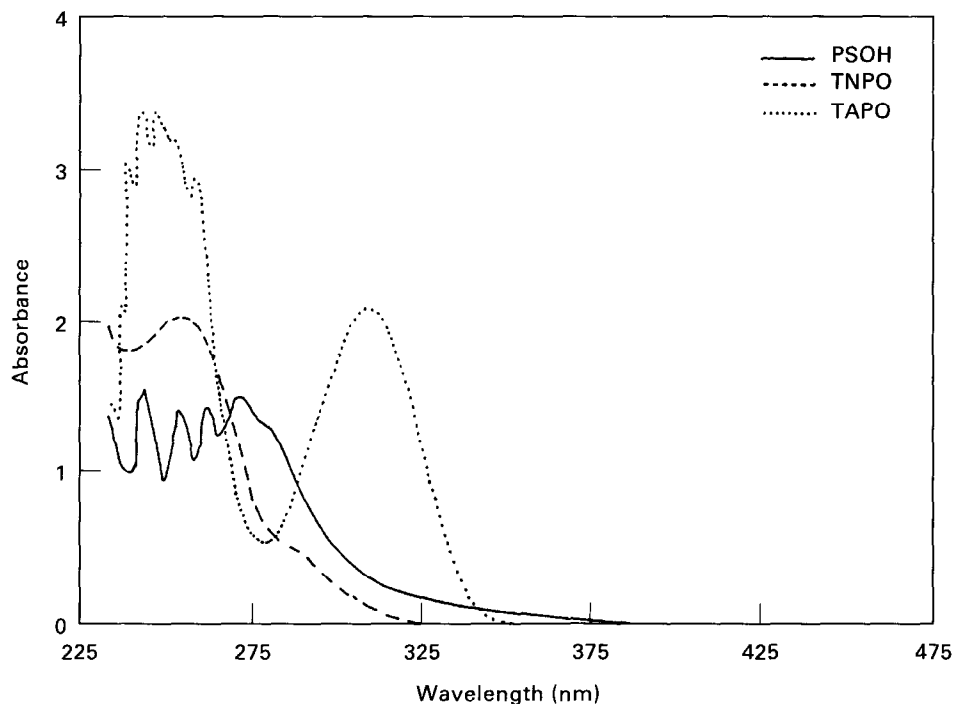

Fig. 2. U.v./vis absorption spectra of samples TNPO, TAPO, and PSOH in THF.
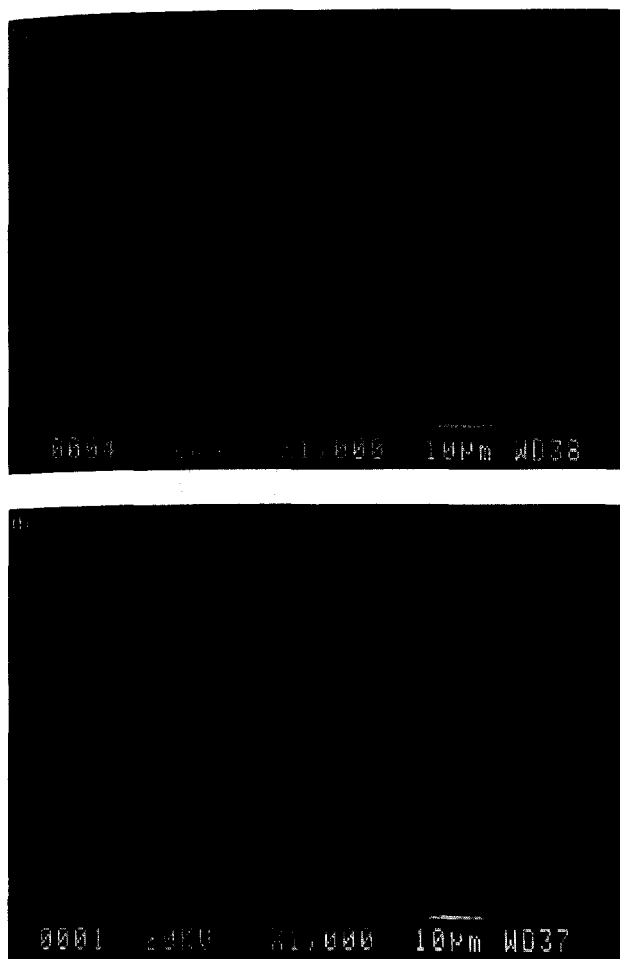
Fig. 3. X-ray elemental maps of samples (a) TNPO10, and (b) TAPO25.

(a)

(b)

(c)

Fig. 4. Dielectric loss tangent versus temperature and frequency for samples (a) PSOH, (b) TNPO10, and (c) TAPO25.

observed at low frequencies (below 10^2 Hz). At higher temperature range, the relaxation was merged into the α-relaxation region. This phenomenon has been reported by McCrum et al. [21]. The α- and β-relaxations were also clearly observed for samples TNPO10 and TAPO25 in Fig. 4(b,c). The relaxation temperatures were shifted to the lower temperature range for these two samples compared to that for the PSOH sample. Moreover, the β-relaxation deviated from the region of the α-relaxation, especially for the TAPO25 sample. The plots of α-relaxation frequency versus temperature for samples PSOH, TNPO10 and TAPO25 are shown in Fig. 5. A non-linear 'WLF' curve of the α-relaxation was obtained for these samples, indicating that the α-relaxation could be identified as the glass transition [22]. The α-relaxation temperature was shifted to the lower temperature range for samples TNPO10 and TAPO25 compared to that for the PSOH sample, due to the plasticizer effect of NLO chromophores. Moreover, the relaxation frequency was increased with increasing content of guest molecules. The existence of the guest molecules in polymer matrix leads to the increase of the intermolecular distance and molecular mobility for samples TNPO10 and TAPO25. As a result of
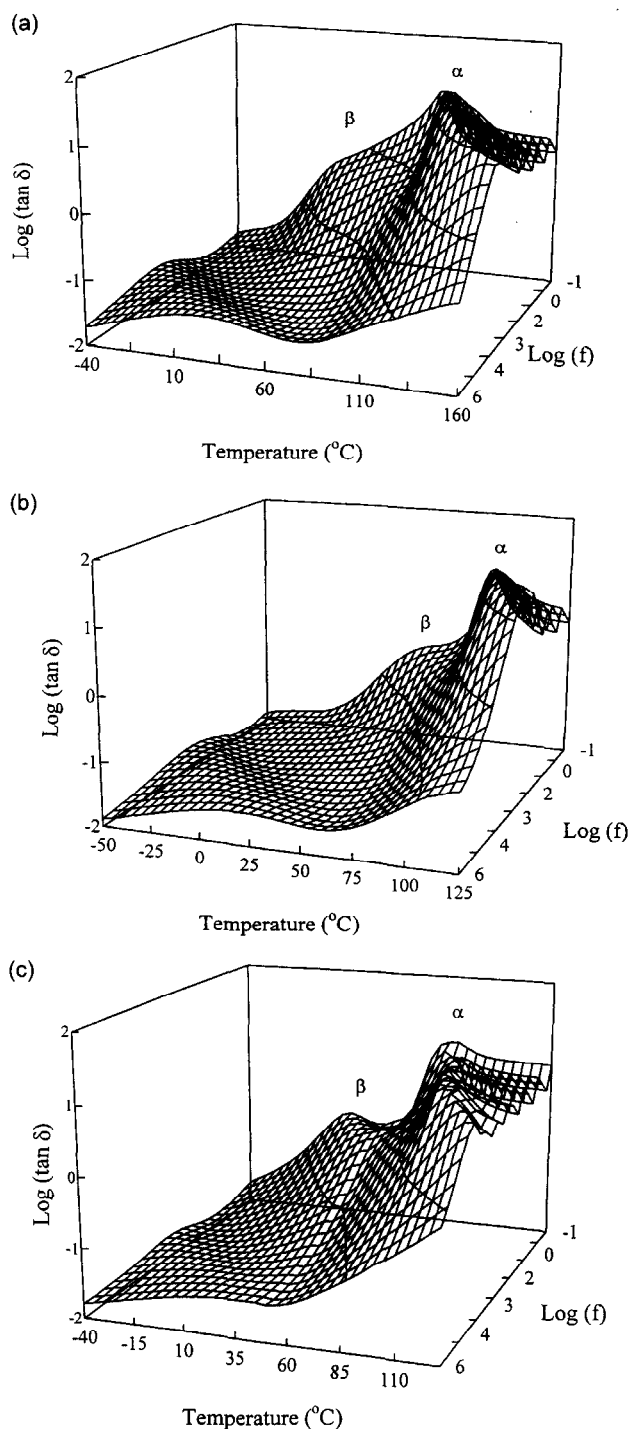
that, a shorter α-relaxation time was obtained for these two guest–host NLO polymeric materials. In addition, the activation energies of the α-relaxation for samples PSOH, TNPO10 and TAPO25 are summarized in Table 1. The activation energy of the α-relaxation was decreased with increasing content of the NLO chromophores due to the plasticizer effect.

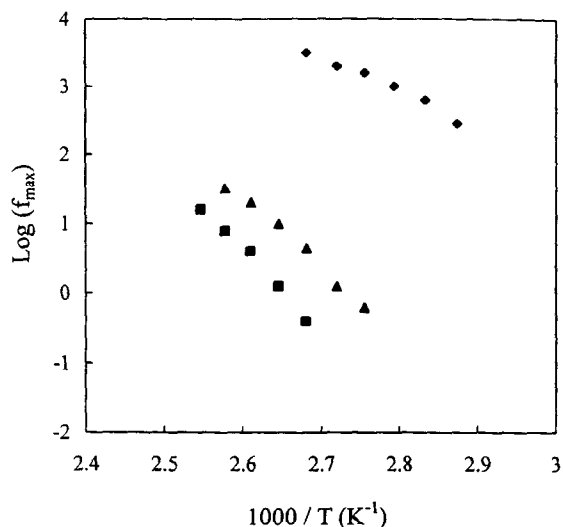The second-order optical nonlinearity was observed for

Fig. 5. Temperature dependence of the relaxation frequencies for the α-relaxation of samples PSOH (■), TNPO10 (▲), and TAPO25 (◆).

Table 1
Activation energies (kJ mol^{-1}) of the α-relaxation[a] for samples PSOH–TAPO25

Sample	α-Relaxation
PSOH	185.3^{b}–281.6^{d}
TNPO10	113.6^{b}–164.1^{d}
TAPO25	78.3^{c}–155.1^{e}

[a] α-Relaxation ± 15 kJ mol^{-1}
[b] Data were calculated at 10 Hz
[c] Data were calculated at $10^{3.5}$ Hz
[d] Data were calculated at $10^{-0.5}$ Hz
[e] Data were calculated at $10^{2.5}$ Hz

the poled guest–host polymers TNPO10 and TAPO25. The poled TNPO10 and TAPO25 samples exhibit d_{33} values of 1.3 and 2.1 pm V^{-1}, respectively. The temporal characteristics of the second harmonic coefficient (d_{33}) for the poled TNPO10 and TAPO25 samples at 35 and 100°C are shown in Fig. 6(a) and Fig. 6(b), respectively. In Fig. 6(a), a reduction of 17 and 23% in d_{eff} value was observed for the poled TNPO10 and TAPO25, respectively, after thermal treatment at 35°C for 1 h. The relaxation of the second harmonic coefficient for the poled TNPO10 and TAPO25 samples at 35°C were affected by the thermal molecular motion of β-relaxation. The β-relaxation for these two NLO guest–host polymers has been observed at room temperature by dielectric spectroscopy. The molecular motion during the β-relaxation leads to a slight relaxation of the second harmonic coefficient at 35°C for poled TNPO10 and TAPO25 samples. In addition, the second harmonic coefficient decayed remarkably for the poled TNPO10 and TAPO25 at 100°C (Fig. 6(b)). The relaxation of second harmonic coefficient was affected by the molecular motion of the α-relaxation for these two NLO polymers at 100°C. Moreover, the TAPO25 sample has a shorter relaxation time
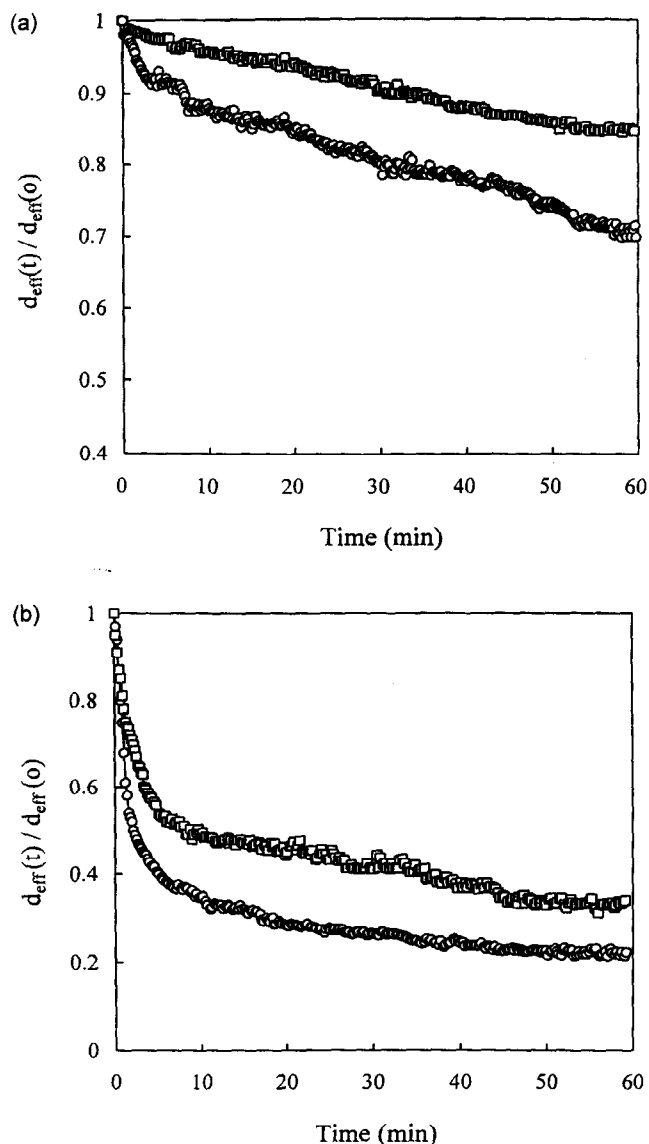

Fig. 6. Temporal behaviour of the effective second-order NLO coefficient of the poled samples TNPO10 (□), and TAPO25 (O): (a) at 35°C, (b) at 100°C for 1 h.

and smaller activation energy of α-relaxation compared to that of the TNPO10 sample by dielectric measurement. This implies that the TAPO25 sample has a higher molecular mobility during the α-relaxation than TNPO10 sample. Because of that, the poled TNPO10 has a better temporal stability of second-order optical nonlinearity than the poled TAPO25 sample at elevated temperature.

4. Conclusion

Novel second-order NLO guest–host polymeric materials based on arylphosphine oxides and PSOH have been developed. This guest–host system exhibits optical transparency down to 400 nm, which is desirable for application in frequency doubling. The homogeneity of these two

guest–host NLO polymers was confirmed using SEM. The result indicates that the guest molecules are distributed uniformly in the polymer matrix for the guest–host polymeric systems. A high doping level (25% by weight) is achieved without occurrence of aggregation. This is possibly due to the intermolecular hydrogen bonding between the NLO chromophores and PSOH. The poled TNPO10 and TAPO25 samples exhibit d_{33} values of 1.3 and 2.1 pm V^{-1}, respectively. The temporal stability of second-order nonlinearity were affected by the α- and β-relaxations for NLO polymers at 100 and 35°C, respectively. A relatively better temporal stability was obtained for poled TNPO10 compared to that for poled TAPO25, due to the more pronounced plasticizer effect in TAPO25.

Acknowledgements

References

[1] Prasad PN, Williams DJ. In: Introduction to nonlinear optical effects in molecules and polymers. New York: Wiley, 1991.

[2] Dalton LR, Harper AW, Ghosn R, Steier WH, Ziari M, Fetterman H, Shi Y, Mustacich RV, Jen AKY, Shea KJ. Chem Mater 1995;7:1060.

[3] Rikken GLJA, Seppen CJE, Nijhuis S, Meijer EW. Appl Phys Lett 1991;58:435.

[4] Nalwa HS, Watanabe T, Kakuta A, Mukoh A, Miyata S. Appl Phys Lett 1993;62:3223.

[5] Cazeca M, Jiang XL, Masse CE, Kamath M, Jeng RJ, Kumar J, Tripathy SK. Opt Commun 1995;117:127.

[6] Nemoto N, Miyata F, Nagase Y, Abe J, Hasegawa M, Shirai Y. J Mater Chem 1996;6:711.

[7] Kott KL, Whitaker CM, McMahon RJ. Chem Mater 1995;7:426.

[8] Ching KC, Lequan M, Lequan RM, Runser C, Barzoukas M, Fort A. J Mater Chem 1995;5:649.

[9] Lequan M, Lequan RM, Ching KC, Bassoul P, Bravic G, Barrans Y, Chasseau D. J Mater Chem 1996;6:5.

[10] Etter MC, Baures PW. J Am Chem Soc 1988;110:639.

[11] Etter MC, Huang KS. Chem Mater 1992;4:824.

[12] Panunto TW, Lipkowska ZU, Johnson R, Etter MC. J Am Chem Soc 1997;109:7786.

[13] Hampsch HL, Yang J, Wong GK, Torkelson JM. Macromolecules 1990;23:3640.

[14] Hsiue GH, Lee RH, Jeng RJ. Chem Mater 1997;9:883.

[15] Jeng RJ, Chen YM, Kumar J, Tripathy SK. J Macromol Sci, Pure Appl Chem 1992;A29:1115.

[16] Mandal BK, Chen YM, Lee JY, Kumar J, Tripathy SK. Appl Phys Lett 1991;58:2459.

[17] Lawes G. In: James AM, editor. Scanning electron microscopy and X-ray microanalysis, Ch. 3. New York: Wiley, 1987:78.

[18] Miller RD, Burland DM, Jurich M, Lee VY, Moylan CR, Thackara JI, Twieg RJ, Verbiest T, Volksen W. Macromolecules 1995;28:4970.

[19] Yu D, Gharavi A, Yu L. Macromolecules 1996;29:6139.

[20] Kohler W, Robello DR, Willand CS, Williams DJ. Macromolecules 1991;24:4589.

[21] McCrum NG, Read BE, Williams G. In: Anelastic and dielectric effects in polymeric solids, Ch. 10. New York: Wiley, 1967:411.

[22] Malmstrom E, Liu F, Boyd RH, Hult A, Gedde UW. Polym Bull 1994;32:679.